Icarus 227 (2014) 176–194

Contents lists available at ScienceDirect

Icarus

journal homepage: www.elsevier.com/locate/icarus

Effects of rocket exhaust on lunar soil reflectance properties

Ryan N. Clegg [a,*], Bradley L. Jolliff [a], Mark S. Robinson [b], Bruce W. Hapke [c], Jeffrey B. Plescia [d]

[a] Washington University in St. Louis, Department of Earth and Planetary Sciences, Campus Box 1169, 1 Brookings Drive, Saint Louis, MO 63130, United States
[b] School of Earth and Space Exploration, Arizona State University, Tempe, AZ 85287, United States
[c] Department of Geology and Planetary Science, University of Pittsburgh, Pittsburgh, PA 15260, United States
[d] Applied Physics Lab, Johns Hopkins University, Baltimore, MD 21218, United States

ARTICLE INFO

Article history:
Received 12 April 2013
Revised 23 August 2013
Accepted 7 September 2013
Available online 23 September 2013

Keywords:
Moon
Moon, surface
Photometry
Image processing

ABSTRACT

High-resolution images of the Surveyor, Luna, and Apollo landing sites obtained by the Lunar Reconnaissance Orbiter Camera (LROC) Narrow Angle Camera (NAC) show regions around the landers where reflectivity of the surface was modified. We interpret the change in reflectance properties of these regions mainly as disturbance of the regolith by rocket exhaust during descent of the spacecraft and we refer to these areas herein as "blast zones" (BZs). The BZs consist of an area of lower reflectance (LR-BZ) compared to the surroundings that extends up to a few meters out from the landers, as well as a broader halo of higher reflectance (HR-BZ) that extends tens to hundreds of meters away from the landers. When approximated as an ellipse, the average Apollo BZ area is $\sim$29,000 m^2 ($\sim$175 ± 60 m by 200 ± 27 m) which is 10× larger than the average Luna BZ, and over 100× larger than the average Surveyor BZ. The LR-BZs are most evident at the Apollo sites, especially where astronaut activity disturbed the soil, leading to a 15–30% (relative to background undisturbed areas) reduction in reflectance at $\sim$30° phase angle. The LR-BZs at the Surveyor and Luna sites are less evident and are unresolvable with NAC images. The average reflectance in the HR-BZs as determined for 30° phase angle is 3–12% higher than in the undisturbed surrounding areas; this magnitude is the same, within uncertainty, for all sites, indicating a common process or combination of processes causing differences in reflectance properties of the regolith. Phase-ratio images and photometric data collected over a range of illumination geometries show that a greater separation in reflectance occurs between the HR-BZs and undisturbed areas at phase angles between 0° and 70° and indicates that the HR-BZs are less backscattering than undisturbed areas. The LR-BZs are affected by macroscopic disruption of the surface and astronaut activity (at the Apollo sites). For the HR-BZ areas, reflectance has likely been affected by scouring from particles entrained by exhaust gases with low-angle trajectories. Regolith particle interactions with surface soil within HR-BZs may destroy fine-scale surface structure (e.g., "fairy-castle") and decrease macroscopic roughness, contributing to a decrease in backscattering character within the HR-BZs and an increase in backscattering character within the LR-BZs. Redistribution of fine particles from the LR-BZ to the HR-BZ may have also contributed to the changed reflectance. Photometric modeling is consistent with one or a combination of these processes.

1. Introduction

The descent engine exhaust plumes of the Surveyor, Luna, and Apollo spacecraft significantly affected the regolith surrounding their landing sites, and owing to the lack of rapid weathering processes on the Moon, these surface alterations are still visible as photometric anomalies in Lunar Reconnaissance Orbiter Camera (LROC) Narrow Angle Camera (NAC) images. These areas, which we refer to as "blast zones" (BZs), are interpreted as disturbances of the regolith by rocket exhaust during descent of the spacecraft and activity of the astronauts in the area right around the landers. Each BZ consists of an area of lower reflectance (LR-BZ) compared to the surroundings that extends from beneath the lander up to a few meters out from the lander, as well as a broader 'halo' of higher reflectance (HR-BZ) that extends tens to hundreds of meters away from the lander (Fig. 1). Kaydash et al. (2011) first discussed the basic phenomenon of BZ reflectance changes; here we present an in-depth analysis of several hypotheses to test possible causes of the reflectance changes. We use photometric modeling, phase-ratio images, and analysis of Apollo sample data to analyze reflectance variations at all of the Apollo sites, as well as at the Luna and Surveyor robotic landing sites.

Disturbed lunar regolith has distinctly different photometric properties compared to undisturbed regolith (Carrier, 1973; Carrier et al., 1991; Hapke, 1981a,b; Kaydash et al., 2011).

* Corresponding author.
E-mail address: rclegg@levee.wustl.edu (R.N. Clegg).

0019-1035/$ - see front matter © 2013 Elsevier Inc. All rights reserved.
http://dx.doi.org/10.1016/j.icarus.2013.09.013

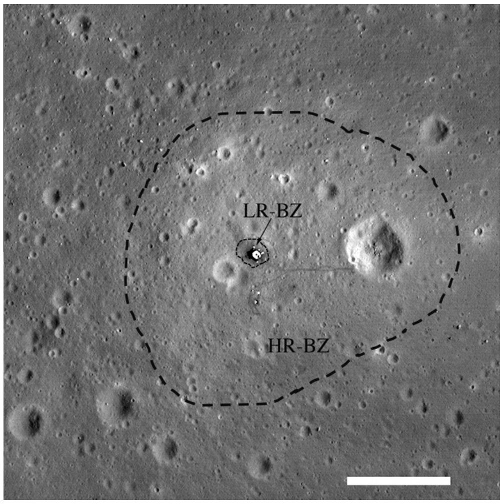

Fig. 1. Apollo 11 landing site, with LR-BZ and HR-BZ outlined. NAC image M175124932LR.

Properties such as grain size, grain shapes, composition and mineralogy, regolith structure, surface roughness, glass and Fe^0 contents determine how the surface reflects light. Lunar regolith properties can be inferred by analyzing the reflectance of the HR-BZs and LR-BZs over a range of incidence, emission, and phase angles from the NAC images. These results can then be compared with the known properties of lunar soils from sample analysis in order to infer the behavior of lunar soil during human and robotic missions (Carrier et al., 1991; Goguen et al., 2010).

The LROC NACs provide high-resolution (50 cm/pixel) images of all the Apollo, Surveyor, and Luna landing sites under a wide variety of illumination conditions (see Appendix A of Supplementary Material), allowing for a detailed photometric analysis of the landing sites. We use photometric analysis of the NAC images to measure the spatial extent of the disturbed areas, as well as to quantify differences in reflectance between the blast zones (both HR-BZs and LR-BZs) and nearby undisturbed regions. This work focuses mainly on the Apollo landing sites because extensive data exist regarding the descent of the lunar modules and the soil behavior around the landing sites. However, we also compare the spatial extent of the BZs and reflectance variations with those seen at the Surveyor and several of the Luna landing sites.

Hypotheses that we consider in this paper to explain the reflectance differences between the HR-BZ and background regions include: (1) change in macroscopic roughness (cm to m scale); (2) redistribution of fine particles (excavation from LR-BZ and deposition to HR-BZ); (3) removal of a more mature surface layer in the HR-BZ and exposure of less mature soil beneath; (4) microscopic (μm scale) modification of fine-scale structure in the HR-BZ (e.g., "fairy castle" structure, see Hapke and van Horn, 1963); (5) compaction of the regolith within the more reflective area; (6) chemical changes due to contamination by the rocket exhaust, and (7) some combination of these effects. We also compare our conclusions with those of recent work by Shkuratov et al. (2013).

2. Methods

NAC images were photometrically corrected and projected to map format using the USGS's Integrated Software for Imagers and Spectrometers (ISIS) (Anderson et al., 2004). We use ISIS to create phase-ratio images, and use both ENVI (Environment for Visualizing Images) and ISIS to analyze NAC images to quantify reflectance properties. In ISIS, the processing step *lronaccal* was used to remove camera artifacts by applying a radiometric calibration to each NAC image. The images were corrected to I/F (Minnaert, 1961), the ratio of the radiance I received at the detector to the radiance from a normally illuminated Lambertian surface F (defined as the source radiance divided by π). The spectral responsivity of each NAC was measured using a monochromater before flight. Once the spectral responsivity was characterized, the DN values could be converted to radiance values. For any given observation, the image count rate (measured in DN/ms) constitutes the spectral radiance of the lunar scene weighted by the NAC responsivity. The weighted mean radiance for the NACs is calculated using the image count rate and spectral responsivity. Using the solar irradiance at a distance of 1 AU, the Sun–Moon distance, spectral responsivity of the NACs, and the image count rate, the weighted radiance I/F for the NACs can be calculated for each pixel. For more details, see Robinson et al., 2010. Higher I/F values correspond to areas of higher reflectance, or to areas where local slopes combined with solar incidence are more reflective.

2.1. Measuring the blast zone spatial extents

Phase-ratio images were created for each landing site to delimit the spatial extent of the disturbed areas and to quantify differences in reflectance and backscattering characteristics within the BZs compared to undisturbed areas. A phase-ratio image is made from two images of the same site with similar incidence angles (i) but with significantly different ($>\sim 20°$ for most pairs) emission angles (e), and thus different phase angles (g), and then dividing the higher phase image by the lower (see Kaydash et al., 2011; Table 1). Fig. 2 shows a schematic of a forward scattering viewing geometry (i and e are on opposite sides of the surface normal; $g \sim i + e$) and a backward scattering viewing geometry (i and e are on the same side of the surface normal; $g \sim |i - e|$); these terms will be used throughout the remainder of the paper. Creating a phase-ratio image using two images of each landing site with different viewing geometries enhances variations associated with disturbance from the landing and astronaut activity, and minimizes influences from small-scale surface topography that existed before and after the landings (Kaydash et al., 2011; Shkuratov et al., 2011). By contrast, images taken at zero phase angle emphasize albedo changes that might be caused by chemical changes or particle size effects (Hapke, 1972). We primarily used images taken in subsequent orbits where the incidence angle was approximately the same but emission angle was varied by slewing the spacecraft, resulting in different phase angles.

Fig. 3 shows an example of a phase-ratio image created for the Apollo 12 landing site. The phase-ratio image provides enhanced contrast between the blast zone and surrounding regolith, thus distinctly revealing the perimeters of the blast zone. This enhanced contrast allows the spatial distribution to be measured more accurately than from the original, individual images. The phase-ratio image also reveals differences in backscattering characteristics of the disturbed region compared to the background undisturbed region. The phase function slope is dominated by light-scattering characteristics of the regolith; in this case a darker region in a phase-ratio image corresponds to a lower phase slope and therefore a region that is less backscattering. Shadowed crater walls in the NAC images appear bright in the phase-ratio image, reflecting changes in illumination geometry (incidence and emission angles) interacting with large-scale topography, and changes in regolith physical properties associated with different parts of the impact craters such as interiors versus rims versus ejecta (Kaydash et al., 2011).

2.2. Reflectance profiles

Reflectance profiles taken across each landing site are used to quantify changes in reflectance between the LR-BZs, HR-BZs, and